END PLATE CONNECTION FOR RECTANGULAR HOLLOW SECTION IN BENDING

Arne Aalberg[a*], Arne M. Uhre[b] and Per Kr. Larsen[a]

[a]*Department of Structural Engineering, Norwegian University of Science and Technology, Norway*
[b]*Department of Structural Engineering, NTNU, and Construction company Gunvald Johansen, Bodø, Norway*
[*]*Corresponding author. E-mail address: arne.aalberg@ntnu.no. Phone number: +47 73594624*

Abstract: This paper investigates the behaviour of an extended end plate connection for rectangular hollow sections subjected to bending moment. The end plate extends on two sides of the RHS and has one bolt on each side. Such connection designs are typically used at the ends of RHS columns in laterally braced building frames. The connection is commonly considered as ideally pinned for end-rotation about the weak axis of the connection, i.e., about the axis through the two bolts, while it is partial-rigid about the other main axis. The objectives of the present study are to obtain data for both the initial bending stiffness and the capacity of the end plate connection for moment about each of the two axes. The results are compared to the predictions of the component method of EN 1993-1-8, which is applicable only for the bending about the connection's strong axis. For the weak axis resistance, classical yield line analysis is used to develop an expression for the moment resistance. The test results are used for a discussion of the stiffness boundaries for joint classification for this particular connection.

1 Introduction

Rectangular and quadratic hollow sections are widely used in steel frames, trusses and girders, and are extensively used as columns in buildings. Connection design for hollow sections ranges from fully welded solutions for large structural elements as lattice girders, to connections designed with plates and bolts for assembling elements at the construction site. A common design of the connection of a hollow section to a concrete foundation, or to other structural elements, is to use an extended end plate welded to the section, and fastening by threaded bars or bolts. Such connections may be designed to be either rotationally rigid and full-strength in moment resistance, semi-rigid and partially- or full-strength, or to function as a pinned connections transferring only shear forces.

The design formulas for end plate connections given in EN 1993-1-8 [1] cover typical beam-to-column connections and column bases for I-section members and gives design formulas for predicting both the connection strength and stiffness. Earlier investigations [2,3] pointed out complications when applying the T-stub capacity models [1] for RHS end plate cases, due to bending of the RHS wall and a shift in the location of the hogging plastic line into the part of the end plate inside the section. It was also shown by [2] that modifications were necessary

for the component stiffness models to yield proper results for the RHS cases. It is the intention of the present investigation to contribute with experimental data and analyses on the behaviour of an extended end plate connections used for RHS sections, and to either modify or extend the component model of [1] to cover the present case or to suggest new models. This includes development of modified yield line model for predicting the end plate resistance for the two directions of the bending moment, as well as new stiffness models for predicting the rotational stiffness of the joint.

The connection studied in the present paper has an end plate extending on two sides of the rectangular hollow section, with one bolt on each side. The connection is depicted in Fig. 1. The results presented here were obtained in a master project at NTNU [4].
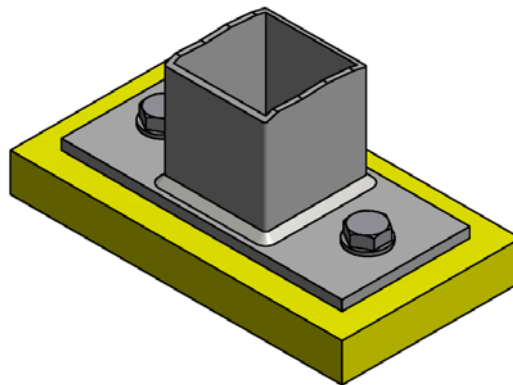

Fig. 1: Investigated end plate connection for RHS member.

2 Test program

A test program was carried out to provide experimental data and to verify the analytical models for joint stiffness and capacity. Results for two specimens are reported in this paper. The test section was a rectangular hollow section RHS 80·80·4 mm in S355. The end plate was also in S355, made from a flat bar with cross-section 100·8 mm. Fig. 2 shows the simple test arrangement. The RHS was fixed to a stiff reaction wall in the laboratory, mounted in a horizontal position as a standard cantilever, and a load (P) was applied at the tip by manual weights. The end plate was connected to the stiff wall by two bolts, as shown in Fig. 2. The connection was tested in two configurations, one with the bolts positioned along a vertical line above and below the horizontal bending axis of the RHS cross-section (Specimen A in Fig.2) and the other with the bolts positioned on the horizontal bending axis (Specimen B). The two test configurations are denoted "strong axis" and "weak axis" in the following, which refers to the moment strength and stiffness of the end plate connection. It is quite obvious that the end plate connection of Specimen A, due to the "correct" orientation of the end plate, is stronger and stiffer than for Specimen B.

The RHS member had a length of approximately 3.0 m in the tests. The end plates had overall dimensions of 220·100 mm and a thickness of 8 mm, and bolt holes positioned as shown in Fig. 3. The measured yield strength of the end plate material was f_y=405 MPa. The specimens were manufactured in the workshop in the laboratory, using ordinary tolerances and weld quality. The throat dimension of the fillet welds varied between 3.7 and 4.2 mm around the section. The bolts were M 16-grade 8.8 in holes 17 mm and were tightened to 80 Nm. The welding introduced an initial curvature in the end plate, which resulted in initial gaps at the plate edges when the end plate was connected to the wall. The chosen bolt pre-tensioning

produced good contact between the end plates in the region around the bolt hole, but a small gap remained at the edges.
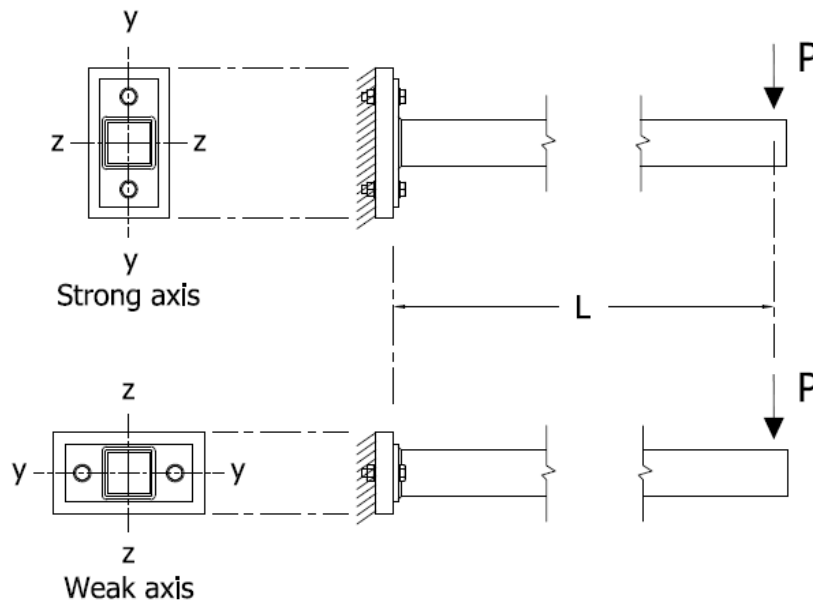

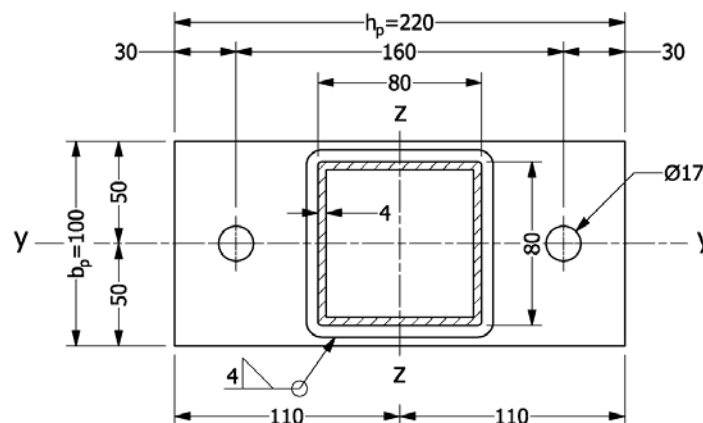**Fig. 2:** Geometry of test specimen A (top) and B (bottom).

Fig. 3: Geometry of end plate.

Several loading-unloading sequences were performed at low load levels in order to obtain accurate data on the initial bending stiffness of the end plate connections. Finally, both specimens were loaded with increasing weights until plastic bending occurred and the connection was permanently deformed. No physical failures were observed, even though the vertical displacement at the tip of the cantilever was 400-500 mm when the tests were terminated. The manual weights and available clearance to the test floor did not allow further loading. After unloading, the remaining displacement at the tip of the cantilever was approximately 250 mm. The permanent deformation occurred in the end plates and by some bending deformation of the bolts.

The weights (P) were applied in increments of 5 kg at the low load levels (initial stiffness range). The bending moment at the joint was calculated from simple statics ($M=P \cdot L$, see Fig. 2). The cantilever displacement was read manually at the load point using a simple tape

measure at each load increment. The rotation of the connection was measured using rotation gauges (Accustar electronic clinometers) attached to the RHS sidewalls adjacent to the weld to the end plate, using a pin and plate arrangement. This can be seen in Fig. 4 (one rotation gauge on the RHS was not mounted yet when the image was taken). A thick support plate was used to attach the tests specimens to the reaction wall, as shown in the image to the left in Fig. 4. A rotation gauge was also mounted on the support plate to check that it was stiff enough not to influence the rotation.

Fig. 4: Support plate on reaction wall (left) and connected Specimen A (right) with rotation gauges.

3 Test results

The test programme is summarized in Table 1.

<div align="center">

Table 1: Test programme

</div>

Test specimen	Moment at initiation of permanent rotation (kNm)	Moment at termination of test (kNm)	Prediction by Yield line analysis (kNm)	Initial connection stiffness $S_{j,ini}$ (kNm/rad)
A	3.0	8	4.55	560
B	2.5	5.3	4.6	180

3.1 Strong axis bending

The response curves obtained in the strong axis bending test (Specimen A) are given in Figs. 5 and 6, with the recorded data points indicated on the curves. Fig. 5 shows the behaviour of the specimen in an initial loading test, where the specimen was loaded to a moment of approximately 2.5 kNm and a corresponding rotation of 0.005 radians. Fig. 6 shows the complete response curve obtained when the specimen was loaded into the inelastic range, where the test was terminated at a load of 280 kg. This caused a maximum moment of 8 kNm at the rotation of 0.1 radians (at 400 mm displacement at the tip of the cantilever).

The rotation recorded by the rotation gauges was compared with the rotation derived from the measured displacements of the tip of the cantilever. This was done by subtracting the deflec-

tion caused by the bending deformation of the cantilever, $\Delta = PL^3 / 3EI$, from the measured displacement and converting the remaining into a concentrated rotation at the connection. The resulting moment-rotation curves (not shown here) were practically identical with those in Figs. 5 and 6 (and similarly in Figs. 8 and 9 for the weak axis test).
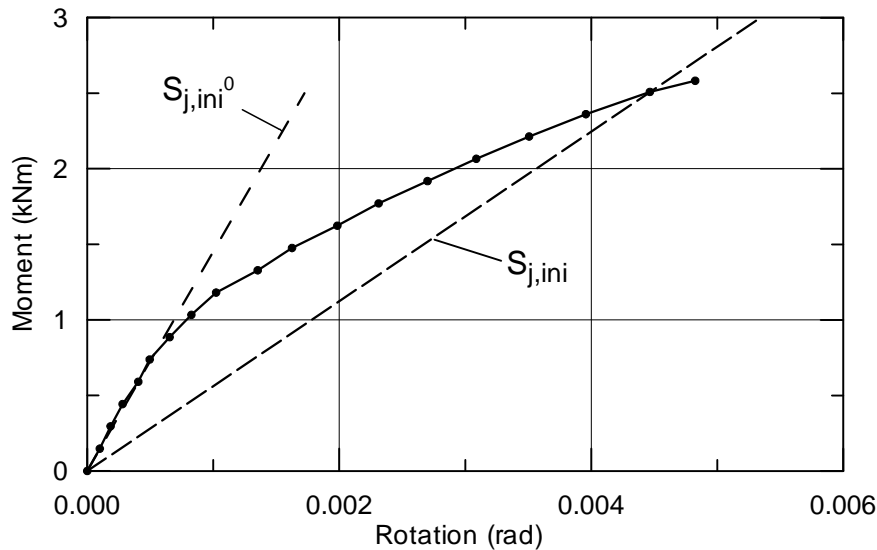

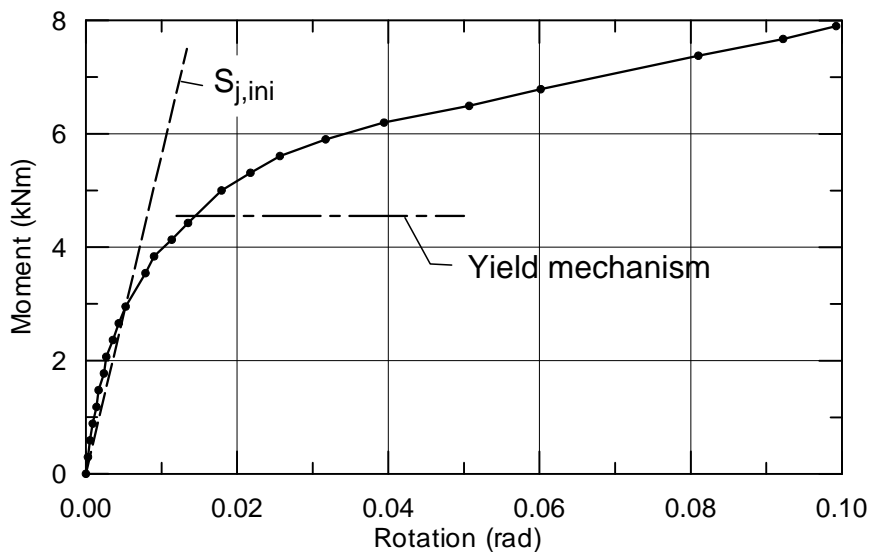**Fig. 5:** Response of Specimen A for initial loading step.

Fig. 6: Response of Specimen A for final capacity test.

In an ideal case the initial part of the response curve would be linear over a significant part of the loading range and the initial (elastic) stiffness of the connection thus easy to define. As seen this is not the case here. Similar observations have been reported by [2,5,6]. The response curve is non-linear from the very beginning of the test. The reason is the complexity of the contact zone / compressed area between the end plate and the support plate. Due to the initial curvature of the end plate and the local contact zone in the region around the pre-tensioned bolts, the contact pressure is non-uniform in both directions (y and z) in the inter-face between the plates. During loading the developed end-rotation of the RHS causes elastic

bending deformations in the end plate, particularly at the tension side of the connection. This causes lever arm and prying action effects and changes the contact area between the plates. At larger moment a gap develops between the end plate and the support plate at the level of the upper wall of the RHS section, which shifts the contact zone between the plates toward the upper edge of the end plate. It was observed at the end of the test that there was still contact at the middle part of the upper edge of the end plate (over a width of 40 mm), but there were significant gaps at the corners of the end plate. At the compression side of the RHS section the largest compressive stresses probably occurred between the end plate and the support plate in the area in line with the bottom wall or the weld of the RHS.

The initial loading and unloading sequences for Specimen A were performed seven times, to increasing load levels (weights) from 30 to 100 kg. Fig. 5 depicts the response curve for a maximum loading of 87.5 kg. For all lower load levels the obtained response curves were practically identical and perfectly elastic, as the rotation returned to zero after the load was removed. As shown in Fig. 5, a straight line S_{ini}^{0} is fitted to the initial part of the response curve. The line corresponds to a connection stiffness of 1450 kNm/rad. It is observed in the figure that this stiffness only reflects the behaviour for moment up to 1.0 kNm, which is far below the actual capacity of the connection, and thus not very relevant.

Some suggestions on how to define the initial rotation stiffness (design stiffness) of the specimen may be found in the definition figure of EN 1993-1-8 (Figure 6.1 and section 6.1.2.3), giving the theoretical moment-rotation relation obtained using the component method. The initial stiffness is defined from the initial linear region of the curve, corresponding to 2/3 of the moment capacity of the joint. The curve has a pronounced "knee" and the joint capacity is given by a constant moment, which enables the simple definition. For the nonlinear curve of the test (Figs. 5 and 6) it was chosen to define the design stiffness by a straight line fitted to the response curve such that it intersected the response curve at the moment corresponding to the initiation of permanent rotation (i.e., secant stiffness). References [5,6] use alternative definitions. For practical reasons the stiffness was derived from the test data using the moment causing a small permanent rotation (10 % of the applied rotation remaining when the loading was removed). For the test specimen this occurred at a moment of approximately 3.0 kNm (Table 1). The constructed stiffness line, $S_{j,ini}$, is shown in Figs. 5 and 6, and has the stiffness value $S_{j,ini}$=560 kNm/rad. As observed in Fig. 6 the line provides a reasonable estimate for the stiffness of the connection for moment up to 50% of the applied maximum moment in the test.

Fig. 7: Deformed end plate of Specimen A, close-up of extending part at tension side.

The image in Fig. 7 shows the deformed shape of the end plate after the test. A yield line has developed across the plate adjacent to the toe of the weld, while the plate is bent in both directions in the region of the bolt. The gap at the corner is clearly visible.

3.2 Weak axis bending

The response curves obtained in the weak axis bending tests (Specimen B) are given in Figs. 8 and 9. The initial loading sequences for this specimen were performed in the same manner as for the strong axis test (Specimen A). It is observed from Fig. 8 that the first part of the response curve is quite linear. The onset of permanent deformations for this specimen occurred at a moment of approximately 2.5 kNm. By defining an initial stiffness and a design stiffness in the same manner as for Specimen A the values S_{ini}^{0}=220 kNm/rad and S_{ini}=180 kNm/rad are obtained, respectively, both indicated in Fig. 8.
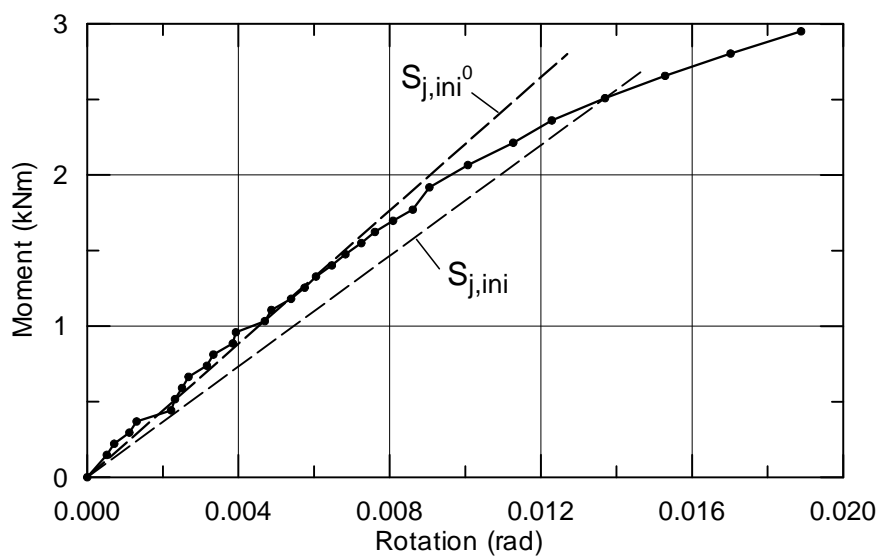

Fig. 8: Response of Specimen B for initial loading step.
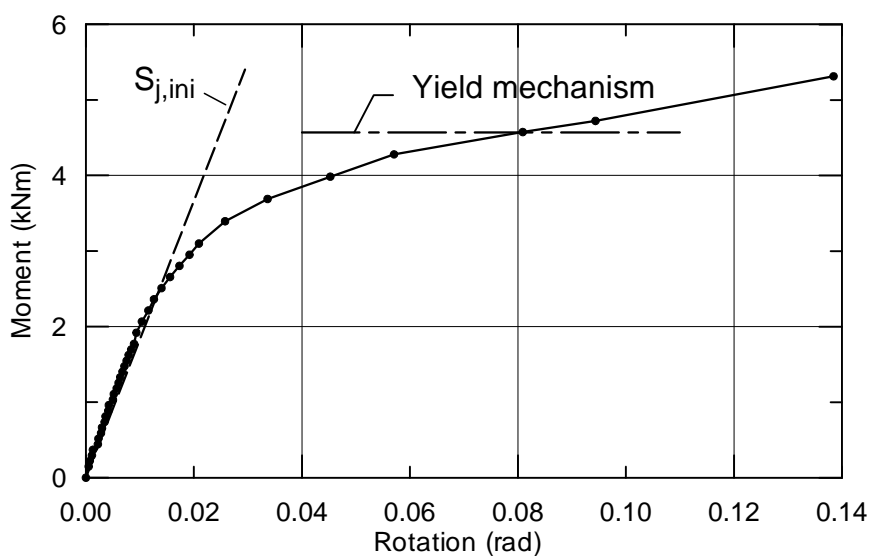

Fig. 9: Response of Specimen B for final capacity test.

The shape of the response curve for the capacity test (Fig. 9) closely resembles that of Specimen A. The largest load applied was 180 kg before the test was terminated, corresponding to a maximum moment of 5.3 kNm and a rotation of 0.135 radians with 460 mm displacement at the cantilever tip.

The images in Fig. 10 show the deformed shape of the specimen in the test rig at 5.3 kNm loading. As seen, there is a gap of several millimetres along the upper edge of the end plate, i.e., at the tension side of the connection. Note that the gap goes all the way to the corners of the plate (image to the right).
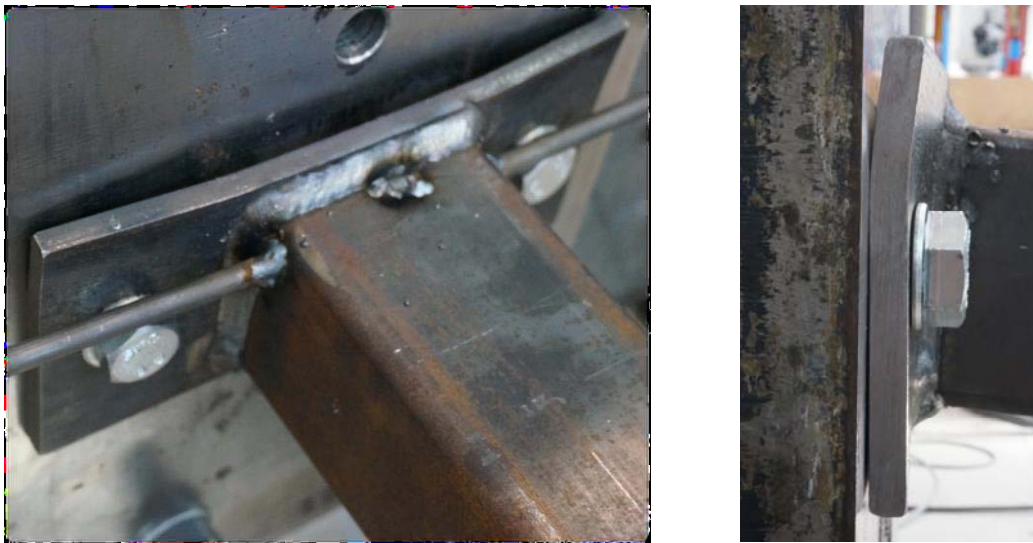

Fig. 10: Deformed end plate connection of Specimen B. Left: view from above. Right: view from the side showing a 5 mm gap at the upper corner of the plate and small gap along the vertical edge of the end plate at the lower part.

4 Comparison with predictions – strong axis bending

As a first attempt to predict the capacity and stiffness of the test specimen for strong axis bending the concept and formulas of Eurocode 3-1-8 [1] were applied. The decisive failure mechanism is a full yield mechanism in end plate with two yield lines at the tension side; one yield line located at the toe of the weld and the other through the bolt hole (Mode 1 of [1]). The extending part of the end plate below the RHS is neglected. The effective length of the model T-stub [1] is thus $b_p/2=50$ mm and the predicted tension resistance of the stub is 37 kN.

Assuming the compression resultant to be located along the center line of the bottom wall of the RHS, the moment arm between the bottom wall and the bolt on the tension side is 118 mm giving a moment capacity of $M_{j,d}=4.3$ kNm for the connection (considering a force couple). As the weld is located along the outside of the RHS, another reasonable assumption for the location of the compression zone could be the center line of the weld, which gives a moment arm of 123 mm between the forces and the resulting moment capacity $M_{j,d}=4.5$ kNm. Note that the moment arm is not defined for end plates with one row of bolts on the tension. For angle flange cleats the arm is given as the distance between the centre of compression to the bolt-row in tension. The theoretically correct in terms of basic statics would be to distinguish between two cases; for failure of the bolts (Mode 3, i.e., zero prying force) the moment arm is

as indicated in [1] the distance to the bolt-row in tension, whereas for Mode 1 and 2 the equilibrium equation should include the moment in the end plate, which reduces the predicted capacity. However, as favourable effect of developed membrane forces will contribute significantly, simplifications may be justified. $M_{j,d}$=4.5 kNm may thus be accepted.

Fig. 11 shows an alternative model for calculating the moment capacity of the end plate connection. In [6] an almost similar model is outlined. A mechanism with three yield lines (I, II and III) in the end plate is assumed (Mode1-type of failure on the tension side), as observed in the test. The coefficient m_p is the yield moment of the plate (m_p=0.25$t_p^2 f_y$). By equating the external and internal virtual work the following expression is obtained for the applied connection moment to cause the plastic collapse:

$$M_p = 2m_p b_p \left[\frac{h_0}{m_x} + 1 \right] \tag{1}$$
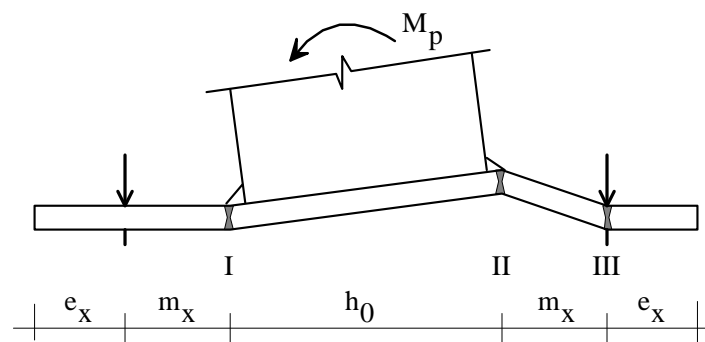

Fig. 11: Yield line model for strong axis bending capacity.

Equation 1 yields a plastic moment capacity of M_p=4.55 kNm. The contribution from yield line I to this value is 14 %. The calculated value of the plastic moment is indicated in Fig. 6 by the horizontal line denoted "yield mechanism". As observed, the moment is located at the level of the diffuse knee-range of the response curve and exceeds the experimental moment corresponding to initiation of permanent rotation in the test (3 kNm) by approximately 1.5 kNm. Compared to the maximum applied moment in the test (8 kNm) the utilization by the predicted plastic moment is modest, as given by the predicted-to-test ratio (M_p/M_{max}) of approximately 0.6. Utilizations on this level for both the classical yield line models (as Eqn. 1) and the formulas of [1] have been reported in several other studies, e.g., [2,6].

The rotational stiffness of the connection predicted by the EN 1993-1-8 model depends on two stiffness coefficients; (1) the coefficient for the axial stiffness of the single bolt on the tension side (k_{10}=0.5·1.6A_s/L_b) and (2) the coefficient for the bending of the extending part of the end plate (k_5=0.9·l_{eff}·t_p^3/m^3). By inserting the values for the bolt and plate dimensions a coupled stiffness (two springs in series) of k=0.42 mm is obtained, which gives a connection stiffness of $S_{j,ini}$=1300 kNm/rad. The plate bending is the major source of the flexibility (77 %). This stiffness agrees quite well with the stiffness in the initial part of the test curve (Fig. 5), where S_{ini}^0= 1450 kNm/rad was determined. The agreement is probably more or less a coincidence and as discussed previously the high initial stiffness S_{ini}^0 is not particularly relevant for the behaviour of this specimen for reasonable moment utilization.

5 Yield line mechanism model for weak axis bending

The deformed end plate of Specimen B was examined after the test in order to determine the shape of the out-of-plane deformations and to establish a capacity model. The plastic deformations in such plates are distributed and do not develop along straight lines; therefore some simplification (judgement?) was necessary. The yield line pattern indicated in Fig. 12a depicts schematically the observed deformations of the specimen (see also images in Fig. 10). However, to enable a kinematic mechanism and simplify the calculations, the model in Fig. 12b is suggested for design purpose. Here, the bolts are assumed without plastic deformations and the yield line pattern is symmetrical on the two sides of the RHS. A vertical yield line (A) is assumed along the side (a-b) of the RHS and another yield line (B) inclined over the end plate through the bolt hole. The RHS may thus rotate along the bottom edge of the end plate. As the edge distance e_x for a normal connection design will be larger than the distance m_x, the inclined yield line (B) may be assumed to extend to edge b-c rather than c-d, which simplifies the problem.
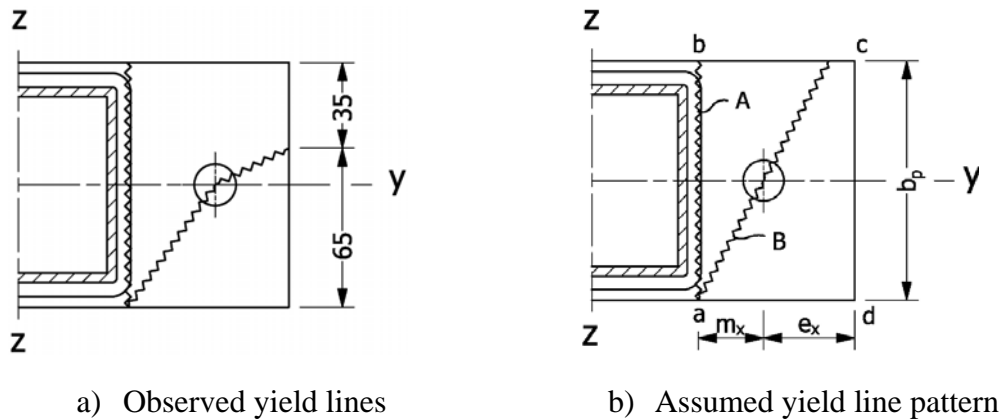

a) Observed yield lines   b) Assumed yield line pattern

Fig. 12: Weak axis bending – yield lines

The equation for the plastic moment M_p of the connection is again determined from the work equations, and is given by

$$M_p = 2\frac{m_p}{m_x}\left[b_p^{\,2} + 2m_x^{\,2}\right] \tag{2}$$

Equation 2 predicts a plastic moment capacity of M_p=4.6 kNm, as indicated in the response plot in Fig. 9. The prediction corresponds for this specimen to a level above the knee-range of the response curve, such that it agrees quite well with the "plastic" region of the curve. The utilization ratio (M_p/M_{max}) is thus higher than observed for the strong axis bending case, Specimen A. One possible explanation for the relatively higher level of the prediction may be connected to the work contributions from the lower part of the assumed yield lines (Fig. 12), where larger rotations of the RHS are required for these regions to become plastified. Besides, there are relatively smaller contributions from membrane forces in the end plate for the weak axis case.

Eurocode 3-1-8 [1] uses the conceptual T-stub to represent the various failure modes that can occur in end plate connections; i.e., the plate yielding failure, combined plate-and-bolt failure and bolt failure (Mode 1 to 3), for either single bolt-rows or groups of bolt-rows. The T-stub

is assigned a finite effective length for each of the failures and has uniform properties along its length. For the present weak axis bending case, the out-of-plane displacements vary over the height of the end plate and it is therefore considered not feasible to assume a uniform T-stub model.

A safe solution to the design problem would be to ensure that the failure modes involving bolt failures are prevented. This may be obtained by ensuring that the bolts have sufficient tensile strength. It is commonly known that the lever arm effect increases the bolt force. In the study of [6], on which the formulas in [1] are based, an increase of 26% in the bolt forces was determined. It is therefore suggested here to design the bolts for a tensile force equal to 1.3 times the force determined directly from the external loading. Assuming the applied moment of the connection to be M_p (Eqn. 2) and that the internal moment arm of the connection is $b_p/2$ (which is the distance from the lower edge of the end plate to the axis through the two bolts in tension), the requirement for the bolt strength becomes (notation as in [1]):

$$F_{t,Rd} = \frac{k_2 f_{ub} A_s}{\gamma_{M2}} \geq F_{t,Ed} = 1.3 \frac{M_p}{b_p} \qquad (3)$$

6 Stiffness boundaries

Classification of stiffness boundaries for joints in building frames are given in section 5.2.2.5 of Eurocode 3-1-8 [1]. The boundaries were established [9-11] to obtain a required accuracy of the design, either with respect to the calculated internal forces and their distribution or the displacements of the structure. A beam-to-column joint can be rigid, semi-rigid or nominally pinned, and it is distinguished between unbraced and braced frames. For column bases only a "rigid-limit" is given, due to the observations [9,10] that all common column bases will have a rotational stiffness higher than what should be classified as nominally pinned.

If the investigated connection detail (Fig. 3) is used for the base of a column of an unbraced frame, the minimum connection stiffness required for it to be classified as rigid would be $30EI_c/L_c$ [1]. Assuming a column length of 2 m the requirement becomes $S_{j,ini}$=3700 kNm/rad. As an illustration, it may be shown that the end plate has to be approximately 14 mm thick to meet the "rigid-limit" requirement, i.e., to have a thickness of 3.5 times that of the wall of the RHS.

For the column base to behave practically as pinned, Birkeland et al. [8] suggested a boundary based on a limit for the moment that can be transmitted by the connection under a realistic rotation. Using 20 % of the moment capacity of the column as limit (same limit as assumed in the derivation of the boundary for the beam-to-column joints), the maximum stiffness allowed becomes $S_{j,ini}$=0.5 EI_c/L_c [11]. This yields a "pinned-limit" of 60 kNm/rad for the present case. The stiffness values observed in the tests were 560 and 180 kNm/rad for the strong and weak axis test, respectively, which are both within the semi-rigid range. The stiffness of the weak axis test is however close to the "ad hock" established pinned-limit. As shown by [8], even a small value of the rotational stiffness of the connection influenced the elastic response of the frame significantly, in particular for the horizontal displacement. Considerations on the effects of simplifications in the joint modelling are thus recommended.

7 Conclusions

The main conclusions are:

1. The investigated RHS end plate connection has a bending moment capacity which may conservatively be assessed by yield line mechanism analysis, both for the strong axis and weak axis bending case.
2. The connection behaves as semi-rigid for a bending moment about the strong axis whereas it is close to pinned for a moment about the weak axis. For the connection to be considered flexurally rigid for moment about the strong axis, an end plate thickness of 3.5 times the RHS wall thickness is necessary.
3. The definition of appropriate initial connection stiffness for elastic analysis should be related to the utilization of the moment resistance of the connection, as the response curve shows nonlinear behaviour even at low load levels.
4. A stiffness model should be developed for the weak axis bending case.

References

[1] EN 1993-1-8:2005, Eurocode 3: "Design of steel structures - Part 1-8: Design of joints", CEN, 2005.
[2] Karlsen, F.T. and Aalberg, A., "Bolted RHS End-Plate Joints in Axial Tension", In: *Proceedings of Nordic Steel Construction Conference* 2012, Oslo.
[3] Packer J.A., Bruno L. and Birkemoe P.C. "Limit analysis of bolted RHS flange plate joints". *Journal of Structural Engineering*, Vol. 115, No.9, 1989.
[4] Uhre, A.M., "Hulprofil med endeplateforbindelse - Hollow Section End Plate Joint" (in Norwegian), Master thesis, Department of Structural Engineering, Norwegian University of Science and Technology (NTNU), June 2013.
[5] Girao, A.M., Bijlaard F.S.K., da Silva L.S. "Experimental assessment of the ductility of extended end plate connections*", Engineering Structures* 26 (2004).
[6] Wheeler A.T. et al., Design model for bolted end plate connections using rectangular hollow sections. Dep of civ engineering, University of Sydney, N.S.W., Australia, 1997.
[7] Weynand K., Jaspart J.P., Steenhuis M. "The stiffness model of revised annex J of Eurocode 3", *Proceedings of the 3rd International Workshop on Connections* (Eds.: R. Bjorhovde, A. Colson, R. Zandonini), Trento, Itália, 441-452, 1995.
[8] Birkeland, I., Aalberg, A., Kvam, S., "Classification Boundaries for Stiffness of Beam-to-Column Joints and Column Bases", In: *Proceedings of Nordic Steel Construction Conference* 2012, Oslo.
[9] Zoetemeijer, P. "A design method for the tension side of statically loaded, bolted beam-to-column connections", *HERON* 20 (1974).
[10] Bijlaard, F.S.K and Steenhuis, C.M. "Prediction of the influence of connection behaviour on the strength, deformations and stability of frames, by classification of connections". Bjorhovde, et al. *Connections in Steel Structures II*. Chigaco : American Institute of Steel Construction, 1992.
[11] Wald, F. et al**.** "Steel column base classification". *HERON*, 53, 2008.